Microresonators Fabricated from High-Kinetic-Inductance Aluminum Films

Wenyuan Zhang, K. Kalashnikov, Wen-Sen Lu, P. Kamenov, T. DiNapoli, and M.E. Gershenson

Phys. Rev. Applied **11**, 011003 — Published 11 January 2019

DOI: 10.1103/PhysRevApplied.11.011003

Microresonators fabricated from high-kinetic-inductance Aluminum films

Wenyuan Zhang,* K. Kalashnikov,* Wen-Sen Lu,* P. Kamenov, T. DiNapoli, and M.E. Gershenson
Department of Physics and Astronomy, Rutgers University,
136 Frelinghuysen Rd., Piscataway, NJ 08854, USA

We have studied superconducting coplanar-waveguide (CPW) resonators fabricated from disordered films of Aluminum. Very high kinetic inductance of these films, inherent to disordered materials, allows us to implement ultra-short (200 μm at 5GHz resonance frequency) and high-impedance (up to 5 kΩ) half-wavelength resonators. We have shown that the intrinsic losses in these resonators at temperatures $\lesssim 250$ mK are limited by resonator coupling to two-level systems (TLS) in the environment. The demonstrated internal quality factors are comparable with those for CPW resonators made of conventional superconductors. High kinetic inductance and well-understood losses make these disordered Aluminum resonators promising for a wide range of microwave applications which include kinetic inductance photon detectors and superconducting quantum circuits.

I. INTRODUCTION

The development of novel quantum circuits for information processing requires the implementation of ultra-low-loss microwave resonators with small dimensions [1]. Superconducting resonators have become ubiquitous parts of high-performance superconducting qubits [2, 3] and kinetic-inductance photon detectors [4]. An important resource for resonator miniaturization is the kinetic inductance of superconductors, L_K, which can exceed the magnetic ("geometrical") inductance by orders of magnitude in narrow and thin superconducting films [5]. High kinetic inductance translates into a high characteristic impedance Z of the microwave (MW) elements, slow propagation of electromagnetic waves, and small dimensions of the MW resonators. Ultra-narrow wires and thin films of Nb and NbN [4, 6], TiN [7], InOx [8, 9], and granular Al [10] were studied recently as candidates for high-L_K applications.

In this Letter, we present a detailed characterization of the half-wavelength microwave resonators fabricated from disordered Aluminum films. Our interest in high-L_K films was stimulated by the possibility of fabrication of superinductors (non-dissipative elements with microwave impedance greatly exceeding the resistance quantum $R_Q = h/(2e)^2$ [11–13]), and the development of superinductor-based protected qubits [14]. We have fabricated resonators with an impedance Z as high as 5 kΩ, ultra-small dimensions and relatively low losses. The study of the temperature dependences of the resonance frequency f_r and intrinsic quality factor Q_i at different MW excitation levels allowed us to identify resonator coupling to TLS in the environment as the primary dissipation mechanism at $T \lesssim 250$ mK; at higher temperatures the losses can be attributed to thermally excited quasiparticles.

II. EXPERIMENTAL DETAILS

The standard method for the fabrication of disordered Al films is the deposition of Al at a reduced oxygen pressure [15, 16]. We have fabricated the films by DC magnetron sputtering of an Al target in the atmosphere of Ar and O_2. The fabrication details are provided in the Supplementary Materials [17]. The films were deposited onto the intrinsic Si substrates at room temperature. By controlling the deposition rate and O_2 pressure, the resistivity of the studied films can be tuned between 10^{-4} Ω·cm and 10^{-1} Ω·cm; the parameters of several representative samples are listed in Table I.

The hybrid microcircuits containing the CPW half-wavelength resonators coupled to a CPW transmission line (TL) have been fabricated using e-beam lithography. The 50-Ω TL was fabricated by the e-gun deposition of a 140-nm-thick film of pure Al on a pre-patterned substrate and successive lift-off. The use of pure Al facilitated the impedance matching with the MW set-up and reduced the number of spurious resonances. After the second e-beam lithography, several half-wavelength disordered Al resonators were fabricated in the openings in the ground plane. The width of the central strip of the resonators varied between 0.5 μm and 10 μm, and the strip-ground distance was fixed at 4 μm.

For the resonator characterization at ultra-low temperatures, we used a microwave setup developed for the study of superconducting qubits [13, 17]. The resonators were designed with the resonance frequencies $f_r \approx 2-4$ GHz, which allowed us to probe the first three harmonics of the resonators within the setup frequency range $(2 \div 12)$ GHz. In order to ensure accurate extraction of the internal quality factor Q_i, the resonators were designed with a coupling quality factor Q_c of the same order of magnitude as Q_i.

III. MICROWAVE CHARACTERIZATION

The resonators were characterized using a wide range of MW power P_{MW}, two-tone (pump-probe) measure-

* These authors contributed equally to this work.

ments, and time domain measurements. The resonator parameters f_r, Q_i, and Q_c were found from the simultaneous measurements of the amplitude and the phase of the transmitted signal $S_{21}(f)$ using the procedure described in Refs. [18, 19] and Supplementary Materials [17]. The kinetic inductance L_K of the central conductor of the resonators, which exceeded the magnetic inductance by several orders of magnitude, was calculated as $L_K = 1/4f_r^2C$ (the capacitance C between the resonator strip and the ground was obtained in the Sonnet simulations).

The measured sheet kinetic inductance $L_{K\square} \approx 2$ nH/$\square$ is similar to that reported for granular Al films in Ref. [20] and TiN in Ref. [21], and exceeds by a factor-of-2 $L_{K\square}$ of ultra-thin disordered InOx films [8, 22]. For the disordered Al films with $\rho < 10$ $m\Omega$·cm, $L_{K\square}$ is in good agreement with the result of the MB theory [23], $L_{K\square}(T=0) = \hbar R_\square/\pi\Delta(0)$, where $\Delta(0)$ is the BCS energy gap at $T = 0$ K. Very large values of $L_{K\square}$ allowed us to realize the characteristic impedance $Z = \sqrt{L_K/C}$ as high as 5 kΩ for the resonators with narrow ($w = 0.7$ μm) central strips. The speed of propagation of the electromagnetic waves in such resonators does not exceed 1% of the speed of light in free space; accordingly, their length is two orders of magnitude smaller than that for the conventional CPW resonators with the impedance $Z = 50$ Ω.

To identify the physical mechanisms of losses in the resonators, we measured the dependences of f_r and Q_i on the temperature ($T = 25 \div 450$ mK) and the microwave power P_{MW}. Below we show that in the case of moderately disordered films (resonators $\#2-4$), both the dissipation and dispersion at $T < 0.25$ K can be attributed to the resonator coupling to the TLS [24] in the environment, whereas at higher temperatures they are controlled by the T dependence of the complex conductivity of superconductors, $\sigma(T) = \sigma_1(T) - i\sigma_2(T)$ [23].

TABLE I. Summary of the measured parameters of AlO_x resonators

#	w, μm	l, μm	f_r, GHz	ρ, mΩ·cm	T_c, K	L_K, nH/$\square$	Z, $k\Omega$
1	11.0	1090	2.42	19.2	1.4	2.0	0.6
2	7.4	765	4.05	4.2	1.7	1.2	1.1
3	1.4	445	3.69	4.2	1.7	1.2	2.9
4	0.7	265	3.88	9.9	1.75	2.0	5.0

A. The resonance frequency analysis

We start the data analysis with the non-monotonic temperature dependence of the relative shift of the resonance frequency $\delta f_r(T)/f_{r0} \equiv [f_r(T) - f_r(25mK)]/f_r(25mK)$. Figure 1(a) shows the dependences $\delta f_r(T)/f_{r0}$ measured for three resonators ($\#2-4$) with different width w. The non-monotonic character of these dependences is due to competing effects of TLS [25] and thermally-induced quasiparticles on f_r. The low-temperature part of $\delta f_r(T)/f_{r0}$ is governed by the T-dependent TLS contribution to the imaginary part of the complex dielectric permittivity $\epsilon(T) = \epsilon_1(T) + i\epsilon_2(T)$. It should be noted that, in contrast to the TLS-related losses, the frequency shift δf_r^{TLS} is expected to be weakly power-dependent [26]. Indeed, the temperature dependences measured for the different values of P_{MW} almost coincide; this simplifies the analysis and reduces the number of fitting parameters. The low-temperature part of $\delta f_r^{TLS}(T)$ is well described by the following equation [4]:

$$\frac{\delta f_r^{TLS}(T)}{f_{r0}} = \frac{V_f\delta_0}{\pi}\left[\Psi_\Re\left(\frac{1}{2} + \frac{1}{2\pi i}\frac{hf_r}{k_BT}\right) - \ln\left(\frac{hf_r}{k_BT}\right)\right]. \quad (1)$$

Here $\Psi_\Re(x)$ is the real part of the complex digamma function, the TLS participation ratio V_f is the energy stored in the TLS-occupied volume normalized by the total energy in the resonator, and the loss tangent δ_0 characterizes the TLS-induced microwave loss in weak electric fields at low temperatures $k_BT \ll hf_r$. The product $V_f\delta_0$ is the only fitting parameter, its values are listed in Table II. The obtained values of $V_f\delta_0$ are close to that found for Al-based [26] and AlO_x-based resonators [21, 27]. Resonator $\#4$ demonstrates the most pronounced increase of $f_r(T)$ with temperature due to the stronger electric fields and a larger participation ratio characteristic of the high-Z resonators [28].

At $T > 0.25$ K, f_r rapidly drops due to the decrease of the superfluid density. The dependences $\delta f_r(T)$ over the whole studied T range can be described as

$$\delta f_r(T)/f_{r0} = \delta f_r^{TLS}(T)/f_{r0} + \delta f_r^{MB}(T)/f_{r0} \quad (2)$$

where

$$\frac{\delta f_r^{MB}(T)}{f_{r0}} = \frac{1}{2}\left[\frac{\sigma_2(T) - \sigma_2(25mK)}{\sigma_2(25mK)}\right] \quad (3)$$

is the resonance shift due to the T-induced break of Cooper pairs and subsequent increase of the kinetic inductance, calculated in the thin film limit [26]. The only free parameter in $\delta f_r^{MB}(T)/f_{r0}$ is the gap energy $\Delta(0)$, which can be found by fitting of the high-T portion of $\delta f_r(T)/f_{r0}$ [Eq. (2)]; the measured ratio $\Delta(0)/T_c$ is about 10% greater than the BCS value of $1.76k_B$, which is consistent with previously reported data [29].

B. The quality factor analysis

We now proceed with the analyses of losses. We observed the enhancement of the internal quality factor Q_i with increasing the average number of photons in the resonators, $\bar{n} = 2P_{MW}Q_l^2/(Q_chf_r^2)$ [30], where $Q_l = (1/Q_i + 1/Q_C)^{-1}$ is the loaded quality factor. The dependences $Q_i(\bar{n})$ for three resonators with different w measured at the base temperature ≈ 25 mK are shown in

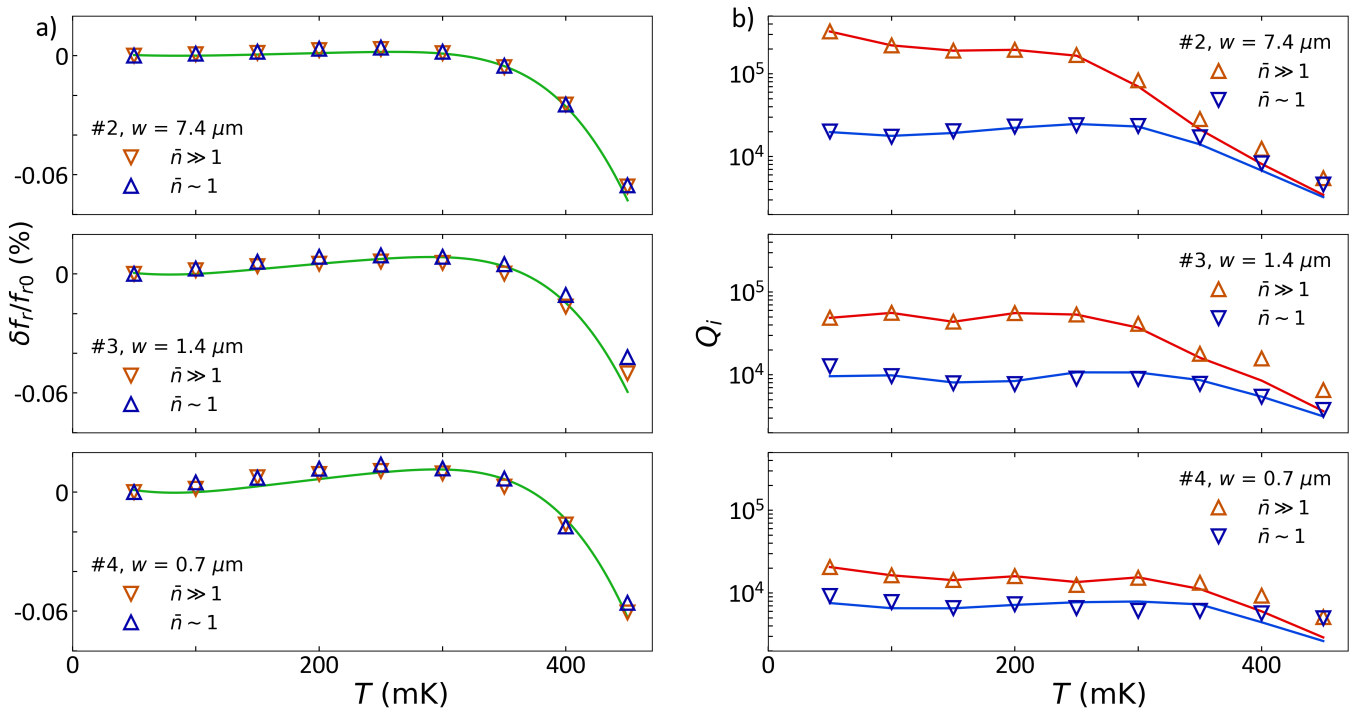

FIG. 1. The temperature dependences of resonance frequency shift $\delta f_r^{TLS}(T)/f_{r0}$ (a) and the internal quality factor Q_i (b) for the resonators $\#2-4$ measured at $\bar{n} \approx 1(\bigtriangledown)$ and $\bar{n} \gg 1(\bigtriangleup)$. The fitting curves correspond to Eq. (2) and Eq. (7), respectively.

Fig. 2. Similar behavior of $Q_i(\bar{n})$ have been observed for many types of CPW superconducting resonators (see, e.g. [4, 31] and references therein), including the resonators based on disordered Al films [10, 20]. The increase of Q_i with the input MW power P_{MW} is limited by the resonance distortion by bifurcation at $P_{MW} > P_*$. For the resonators with $Q_l \gtrsim 10^4$ the onset of bifurcation is observed for the microwave currents $I_* = \sqrt{2P_*/Z}$ which scale approximately as $I_{dp}/\sqrt{Q_l}$ [32], where I_{dp} is the Ginzburg-Landau depairing current in the central strip [17].

The power-dependent intrinsic losses can be attributed to the resonator coupling to the TLS with the Lorentzian-shaped distribution

$$g(E_{TLS}) \sim \frac{1}{(E_{TLS} - hf_r)^2 + (\hbar/\tau_2)^2}, \qquad (4)$$

where E_{TLS} is the energy of TLS and τ_2 is its dephasing time [33]. Once the MW power P_{MW} reaches some characteristic level P_c and the Rabi frequency of the driven TLS $\Omega_R \sim \sqrt{P_{MW}}$ exceeds the relaxation rate $1/\sqrt{\tau_1\tau_2}$, the population of the excited TLS increases, and the amount of energy that the TLS with $f_{TLS} \approx f_r$ can absorb from the resonator decreases. Thus, the high P_{MW} "burns the hole" in the density of states (DoS) of dissipative TLS. The width of the "hole" is $\kappa/2\pi\tau_2$, the power-dependent factor can be written as

$$\kappa = \sqrt{1 + \left(\frac{\bar{n}}{n_c}\right)^{\beta}}, \qquad (5)$$

where $\bar{n}$ and n_c correspond to P_{MW} and P_c, respectively. The exponent β is known to be dependent on the electric field distribution in a resonator [34], and the characteristic power n_c increases with temperature by orders of magnitude due to a strong T-dependence of τ_1 and τ_2 [35, 36]. Taking into account the TLS saturation at high temperature, the power dependence of the TLS-related part of the loss tangent can be expressed as follows [28]:

$$\delta_{TLS}(\bar{n}, T) = \frac{V_f\delta_0}{\kappa} \tanh\left(\frac{hf_r}{2k_BT}\right). \qquad (6)$$

By fitting the experimental data with Eq. (6) we found β and n_c listed in Table II. We found that larger values of β correspond to wide strips, and the extracted $n_c(0)$ scales as the square of the electric field on the surface of the resonator. The details of the fitting procedure can be found in Supplementary Materials [17].

The experimental dependences $Q_i(T)$ measured for resonators $\#2-4$ at $\bar{n} \backsimeq 1$ and $\bar{n} \gg 1$ [Fig. 1(b)] are well described by the sum of the TLS contribution [Eq. (6)] and the MB term $\delta_{MB} = \sigma_1(T)/\sigma_2(T)$ [26]:

$$Q_i(T) = \{\delta_{TLS}(T, \beta, n_c, V_f\delta_0) + \delta_{MB}[T, \Delta(0)]\}^{-1}. \qquad (7)$$

The agreement of measured Q_i with the prediction of Eq. (7) over the whole measured temperature range proves that the losses in the developed resonators are limited by the sum of TLS and MB terms.

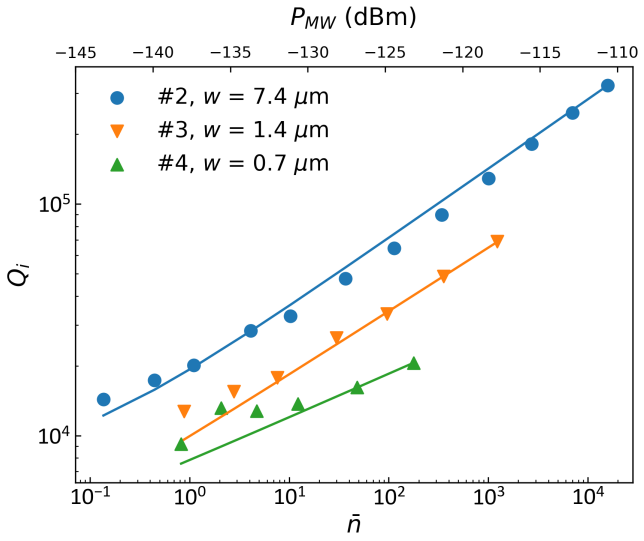

FIG. 2. The dependences $Q_i(\bar{n})$ at $T \approx 25$ mK for the resonators with different widths. Solid curves represent the theoretical fits of the quality factor governed by TLS losses [Eq. (5), see the text for details].

C. The two-tone and time-domain measurements

We obtained an additional information on the TLS-related dissipation by performing the pump-probe experiments in which Q_i was measured at a low-power ($n \backsimeq 1$) probe signal while the power P_p of the pump signal at the frequency f_p was varied over a wide range. Figure 3(a) shows the dependences $Q_i(P_p)$ measured at different detuning values $\Delta f = f_p - f_r = 0, \pm 1$ MHz, and ± 10 MHz. We have not observed any changes in Q_i when the pump signal was applied at the second and third harmonics of the resonator. Also, Q_i was P_p-independent when we monitored the second harmonic and applied the pump signal at the first harmonic.

Since the resonator coupling to the pump signal varies by several orders of magnitude within the detuning range $0 \div 10$ MHz, it is more informative to analyze Q_i as a function of the average number of the "pump" photons in the resonator, $\bar{n}_p = P_p(1-|S_{21}(f_p)|^2-|S_{11}(f_p)|^2)/hf_p^2$, where S_{21} and $S_{11} = 1 - S_{21}$ are the transmission and reflection amplitudes at the pump frequency, respectively. The dependence Q_i on the detuning Δf for a fixed $\bar{n}_p \approx 1000$ is depicted in Fig. 3(b). The resonance behavior of $Q_i(\Delta f)$ is expected since only a narrow TLS band [Eq. (4)] contributes to dissipation: the "hole" extension in the DoS is limited by $\sim \kappa/\tau_2$ around the pump frequency. Indeed, using the approach developed in [37], one can obtain the following expression:

$$Q_i(\Delta) = Q_0\left[1 + \frac{(\kappa/2\pi\tau_2)^2}{\Delta f^2 + \kappa(1/2\pi\tau_2)^2}\right], \qquad (8)$$

where Q_0 is the off-resonance quality factor, and introduced by Eq. (5) factor κ might be calculated as $\kappa = Q_{max}/Q_0$. The dephasing time is the only fitting parameter and it is found to be $\tau_2 \approx 60$ ns. This result agrees with the measurements of the dephasing time for individual TLS in amorphous Al_2O_3 tunnel barrier in Josephson junctions [38].

TABLE II. Summary of the fitting parameters

#	$\Delta(0)/k_BT_c$	β	$V_f\delta_0 \cdot 10^{-4}$	$n_c(0)\cdot 10^{-3}$
2	1.96	0.60	1.4	50
3	1.98	0.55	4.8	1.6
4	1.88	0.38	6.7	0.23

By application of the MW pulses at the pump frequency, we observed that the characteristic time at which Q_i varies with P_p does not exceed 36 ms (see Supplementary Materials [17] for details). For several resonators we have observed the telegraph noise in the resonance frequency on the time scale of $1 - 10$ s. This noise can be attributed to interactions of the resonators with a small number of strongly coupled TLS.

IV. SUMMARY

In conclusion, we have fabricated CPW half-wavelength resonators made of strongly disordered Al films. Because of the very high kinetic inductance of these films, we were able to significantly reduce the length of these resonators, down to $\sim 1\%$ of that of conventional CPW resonators with a 50 Ω impedance. Due to ultra-small dimensions and relatively low losses at mK temperatures, these resonators are promising for the use in quantum superconducting circuits operating at ultra-low temperatures, especially for the applications that require numerous resonators, such as multi-pixel MKIDs [4, 32]. The high impedance $Z = \sqrt{L_K/C}$ of the narrow resonators can be used for effective coupling of spin qubits [39, 40].

We have shown that the main source of losses in these resonators at $T \ll T_c$ is the coupling to the resonant TLS. A comparison of our results with those of the other groups shows that the obtained Q_i values, increasing from $(1 \div 2) \times 10^4$ in the single-photon regime to $3{\times}10^5$ at high microwave power, are typical for the CPW superconducting resonators with similar TLS participation ratios. This implies that the disorder in Al films does not introduce any additional, anomalous losses. Most likely, the relevant TLS are located near the edges of the central resonator strip either in the native oxide on the Si substrate surface or in the amorphous oxide covering the films. Further increase of Q_i can be achieved by the methods aimed at the reduction of surface participation, such as substrate trenching (see [41] and references within) and increasing the gap between the center conductor and the ground plane [34]. The evidence for that was provided by the results of Ref. [20] obtained for the

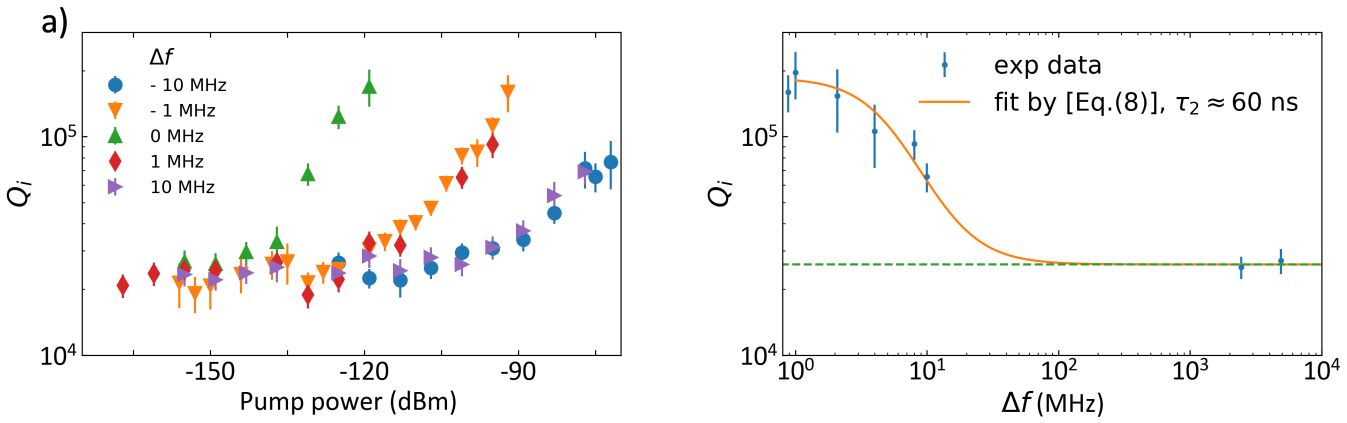

FIG. 3. (a) The dependences of Q_i for resonator #1 on the pump tone power P_p for several values of detuning Δf between resonance and pump frequencies. (b) The values of Q_i measured versus detuning Δf at a fixed number of the pump tone photons in the resonator $\bar{n}_p \approx 1000$. The error bars are derived from the covariance matrix obtained from nonlinear fitting of the measurement of $S_{21}(f)$.

modified three-dimensional microstrip structures based on disordered Al films. It is also worth mentioning that the losses can be reduced using TLS saturation by the microwave signal outside of the resonator bandwidth but within the TLS spectral diffusion range.

ACKNOWLEDGMENTS

This work was supported by the NSF award 1708954.

[1] M. H. Devoret and R. J. Schoelkopf, "Superconducting circuits for quantum information: An outlook," Science **339**, 1169–1174 (2013).

[2] H. Paik, D. I. Schuster, L. S. Bishop, G. Kirchmair, G. Catelani, A. P. Sears, B. R. Johnson, M. J. Reagor, L. Frunzio, L. I. Glazman, S. M. Girvin, M. H. Devoret, and R. J. Schoelkopf, "Observation of High Coherence in Josephson Junction Qubits Measured in a Three-Dimensional Circuit QED Architecture," Phys. Rev. Lett. **107**, 240501 (2011).

[3] R. Barends, J. Kelly, A. Megrant, D. Sank, E. Jeffrey, Y. Chen, Y. Yin, B. Chiaro, J. Mutus, C. Neill, P. O'Malley, P. Roushan, J. Wenner, T. C. White, A. N. Cleland, and John M. Martinis, "Coherent josephson qubit suitable for scalable quantum integrated circuits," Phys. Rev. Lett. **111**, 080502 (2013).

[4] J. Zmuidzinas, "Superconducting Microresonators: Physics and Applications," Annu. Rev. Condens. Matter Phys. **3**, 169–214 (2012).

[5] M. Tinkham, *Introduction to superconductivity* (Dover Publications, 2004).

[6] D. Niepce, J. Burnett, and J. Bylander, "High Kinetic Inductance NbN Nanowire Superinductors," (2018), arXiv:1802.01723.

[7] P. C. J. J. Coumou, E. F. C. Driessen, J. Bueno, C. Chapelier, and T. M. Klapwijk, "Electrodynamic response and local tunneling spectroscopy of strongly disordered superconducting TiN films," Phys. Rev. B **88**, 180505 (2013).

[8] O. Dupré, A. Benoît, M. Calvo, A. Catalano, J. Goupy, C. Hoarau, T. Klein, K. Le Calvez, B. Sacépé, A. Monfardini, and F. Levy-Bertrand, "Tunable sub-gap radiation detection with superconducting resonators," Supercond. Sci. Technol. **30**, 045007 (2017).

[9] S. E. de Graaf, S. T. Skacel, T. Hönigl-Decrinis, R. Shaikhaidarov, H. Rotzinger, S. Linzen, M. Ziegler, U. Hübner, H.-G. Meyer, V. Antonov, E. Il'ichev, A. V. Ustinov, A. Ya. Tzalenchuk, and O. V. Astafiev, "Charge quantum interference device," Nat. Phys. **14**, 590–594 (2018).

[10] H. Rotzinger, S. T. Skacel, M. Pfirrmann, J. N. Voss, J. Münzberg, S. Probst, P. Bushev, M. P. Weides, A. V. Ustinov, and J. E. Mooij, "Aluminium-oxide wires for superconducting high kinetic inductance circuits," Supercond. Sci. Technol. **30**, 025002 (2017).

[11] A. J. Annunziata, D. F. Santavicca, L. Frunzio, G. Catelani, M. J. Rooks, A. Frydman, and Daniel E Prober, "Tunable superconducting nanoinductors," Nanotechnology **21**, 445202 (2010).

[12] V. E. Manucharyan, J. Koch, L. I. Glazman, and M. H. Devoret, "Fluxonium: single cooper-pair circuit free of charge offsets." Science **326**, 113–6 (2009).

[13] M. T. Bell, I. A. Sadovskyy, L. B. Ioffe, A. Yu. Kitaev, and M. E. Gershenson, "Quantum Superinductor with Tunable Nonlinearity," Phys. Rev. Lett. **109**, 137003 (2012).

[14] M. T. Bell, W. Zhang, L. B. Ioffe, and M. E. Gershenson, "Spectroscopic Evidence of the Aharonov-Casher Effect in a Cooper Pair Box," Phys. Rev. Lett. **116**, 107002 (2016).

[15] G. Deutscher, H. Fenichel, M. Gershenson, E. Grünbaum, and Z. Ovadyahu, "Transition to zero dimensionality

in granular aluminum superconducting films," J. Low Temp. Phys. **10**, 231–243 (1973).
[16] K. C. Mui, P. Lindenfeld, and W. L. McLean, "Localization and electron-interaction contributions to the magnetoresistance in three-dimensional metallic granular aluminum," Phys. Rev. B **30**, 2951–2954 (1984).
[17] See Supplemental Material at [URL] for details on experimental methods and data analysis.
[18] M. S. Khalil, M. J. A. Stoutimore, F. C. Wellstood, and K. D. Osborn, "An analysis method for asymmetric resonator transmission applied to superconducting devices," J. Appl. Phys. **111**, 054510 (2012).
[19] S. Probst, F. B. Song, P. A. Bushev, A. V. Ustinov, and M. Weides, "Efficient and robust analysis of complex scattering data under noise in microwave resonators," Rev. Sci. Instrum. **86**, 024706 (2015).
[20] L. Grünhaupt, N. Maleeva, S. T. Skacel, M. Calvo, F. Levy-Bertrand, A. V. Ustinov, H. Rotzinger, A. Monfardini, G.i Catelani, and I. M. Pop, "Quasiparticle dynamics in granular aluminum close to the superconductor to insulator transition," (2018), arXiv:1802.01858.
[21] J. T. Peltonen, P. C. J. J. Coumou, Z. H. Peng, T. M. Klapwijk, J. S. Tsai, and O. V. Astafiev, "Hybrid rf SQUID qubit based on high kinetic inductance," (2017), arXiv:1709.09720.
[22] O. V. Astafiev, L. B. Ioffe, S. Kafanov, Yu. A. Pashkin, K. Yu. Arutyunov, D. Shahar, O. Cohen, and J. S. Tsai, "Coherent quantum phase slip," Nature **484**, 355–358 (2012).
[23] D. C. Mattis and J. Bardeen, "Theory of the Anomalous Skin Effect in Normal and Superconducting Metals," Phys. Rev. **111**, 412–417 (1958).
[24] C. Müller, J. H. Cole, and J. Lisenfeld, "Towards understanding two-level-systems in amorphous solids - Insights from quantum devices," (2017), arXiv:1705.01108.
[25] W. A. Phillips, "Two-level states in glasses," Reports Prog. Phys. **50**, 1657–1708 (1987).
[26] J. Gao, *The physics of superconducting microwave resonators*, Ph.D. thesis (2008).
[27] J. Wenner, R. Barends, R. C. Bialczak, Y. Chen, J. Kelly, E. Lucero, M. Mariantoni, A. Megrant, P. J.J. O'Malley, D. Sank, A. Vainsencher, H. Wang, T. C. White, Y. Yin, J. Zhao, A. N. Cleland, and J. M. Martinis, "Surface loss simulations of superconducting coplanar waveguide resonators," Appl. Phys. Lett. **99**, 99–101 (2011).
[28] J. M. Sage, V. Bolkhovsky, W. D. Oliver, B. Turek, and P. B. Welander, "Study of loss in superconducting coplanar waveguide resonators," J. Appl. Phys. **109**, 063915 (2011).
[29] U. S. Pracht, N. Bachar, L. Benfatto, G. Deutscher, E. Farber, M. Dressel, and M. Scheffler, "Enhanced Cooper pairing versus suppressed phase coherence shaping the superconducting dome in coupled aluminum nanograins," Phys. Rev. B **93**, 100503 (2016).
[30] A. Bruno, G. de Lange, S. Asaad, K. L. van der Enden, N. K. Langford, and L. DiCarlo, "Reducing intrinsic loss in superconducting resonators by surface treatment and deep etching of silicon substrates," Appl. Phys. Lett. **106** (2015).
[31] A. Megrant, C. Neill, R. Barends, B. Chiaro, Y. Chen, L. Feigl, J. Kelly, E. Lucero, M. Mariantoni, P. J. J. O'Malley, D. Sank, A. Vainsencher, J. Wenner, T. C. White, Y. Yin, J. Zhao, C. J. Palmstrøm, J. M. Martinis, and A. N. Cleland, "Planar superconducting resonators with internal quality factors above one million," Appl. Phys. Lett. **100**, 113510 (2012).
[32] L. J. Swenson, P. K. Day, B. H. Eom, H. G. Leduc, N. Llombart, C. M. McKenney, O. Noroozian, and J. Zmuidzinas, "Operation of a titanium nitride superconducting microresonator detector in the nonlinear regime," J. Appl. Phys. **113**, 104501 (2013).
[33] D. P. Pappas, M. R. Vissers, D. S. Wisbey, J. S. Kline, and J. Gao, "Two Level System Loss in Superconducting Microwave Resonators," IEEE Trans. Appl. Supercond. **21**, 871–874 (2011).
[34] H. Wang, M. Hofheinz, J. Wenner, M. Ansmann, R. C. Bialczak, M. Lenander, E. Lucero, M. Neeley, A. D. O'Connell, D. Sank, M. Weides, A. N. Cleland, and J. M. Martinis, "Improving the coherence time of superconducting coplanar resonators," Appl. Phys. Lett. **95**, 233508 (2009).
[35] J. Goetz, F. Deppe, M. Haeberlein, F. Wulschner, C. W. Zollitsch, S. Meier, M. Fischer, P. Eder, E. Xie, K. G. Fedorov, E. P. Menzel, A. Marx, and R. Gross, "Loss mechanisms in superconducting thin film microwave resonators," J. Appl. Phys. **119**, 015304 (2016).
[36] J. Lisenfeld, C. Müller, J. H. Cole, P. Bushev, A. Lukashenko, A. Shnirman, and A. V. Ustinov, "Measuring the Temperature Dependence of Individual Two-Level Systems by Direct Coherent Control," Phys. Rev. Lett. **105**, 230504 (2010).
[37] T. Capelle, E. Flurin, E. Ivanov, J. Palomo, M. Rosticher, S. Chua, T. Briant, P.-F. Cohadon, A. Heidmann, T. Jacqmin, and S. Deleglise, "Energy relaxation properties of a microwave resonator coupled to a pumped two-level system bath," (2018), arXiv:1805.04397.
[38] Y. Shalibo, Y. Rofe, D. Shwa, F. Zeides, M. Neeley, J. M. Martinis, and N. Katz, "Lifetime and Coherence of Two-Level Defects in a Josephson Junction," Phys. Rev. Lett. **105**, 177001 (2010).
[39] N. Samkharadze, A. Bruno, P. Scarlino, G. Zheng, D. P. DiVincenzo, L. DiCarlo, and L. M. K. Vandersypen, "High Kinetic Inductance Superconducting Nanowire Resonators for Circuit QED in a Magnetic Field," Phys. Rev. Appl. **5**, 044004 (2016).
[40] A. Stockklauser, P. Scarlino, J. V. Koski, S. Gasparinetti, C. K. Andersen, C. Reichl, W. Wegscheider, T. Ihn, K. Ensslin, and A. Wallraff, "Strong Coupling Cavity QED with Gate-Defined Double Quantum Dots Enabled by a High Impedance Resonator," Phys. Rev. X **7**, 011030 (2017).
[41] G. Calusine, A. Melville, W. Woods, R. Das, C. Stull, V. Bolkhovsky, D. Braje, D. Hover, D. K. Kim, X. Miloshi, D. Rosenberg, A. Sevi, J. L. Yoder, E. Dauler, and W. D. Oliver, "Analysis and mitigation of interface losses in trenched superconducting coplanar waveguide resonators," Appl. Phys. Lett. **112**, 062601 (2018).